Modeling and Finite Element Validation of a Wind Turbine with a Direct Drive Permanent Magnet Synchronous Generator.

Henda Zorgani Agrebi
Department of Electrical Engineering
National School of Engineering of Gabes
Tunisia
henda.zorganiagrebi@enis.tn

Naourez Benhadj
Department of Electrical Engineering
National School of Engineering of Sfax
Tunisia
naourez.benhadj@enis.tn

Mohamed Chaieb
Departement of Electrical Engineering
National School of Engineering of Chartage
Tunisia
Mohamed.Chaieb@enichartage.tn

Rafik Neji
Departement of Electrical Engineering
National School of Engineering of Sfax
Tunisia
rafik.neji@enis.tn

Abstract

In this paper, the analytical modeling of a wind turbine conversion chain is carried out according to multi-physical disciplines of the system. The chain represents a 3 bladed horizontal axis wind turbine coupled directly to a permanent magnet synchronous generator PMSG delivering power in a battery through a diode rectifier. For the considered chain, four models are developed. Mechanical model describes the power generation from kinetic movement of the wind to its transmission to the generator. Geometric Model clarify the design method of the turbine components. Magnetic Model summarizes the phenomena arising from the influence of the permanent magnets within the generator. Electrical Model determine the parameters and the electrical performance of the machine. Developed models are tested with the Finite Element Analysis FEA to evaluate their reliability. The FEA, by MATLAB-FEMM software, describes the electromagnetic behavior of the PMSG, the main component of the considered simplified chain.

Keywords: Horizontal-Axis Wind Turbine, Analytical Modeling, Direct Drive Permanent Magnet Synchronous Generator, Finite Element Validation.

I. INTRODUCTION

In recent decades, the development of the wind power sector is being a challenge in modern times to supply the global energy needs and to face the ecosystem barriers [1]. By the way, the investment in developing effective models to the wind turbine chain is of vital importance. Analytical modelling intervenes in the elaboration of system optimization models thus they ensure optimal design [2]. It participates in the reliable formulation of dynamic models to describe the system behavior according to wind fluctuations and operating conditions [3]. They allow the analysis of the system from a magnetic and thermal point of view basing on the finite element method [4]. In this way, the development of effective models for a simple wind turbine conversion chain is elaborated. The chain is composed from 3 bladed horizontal axis turbine connected to a gearless synchronous generator with surface permanent magnets having a radial flux and glued to an inner rotor. The choice of such structure is based on several advantages. The absence of the gearbox is considered as an achievement in the wind power generation system offering a higher efficiency with lower vibration and noise and a reduction of the maintenance of the turbine [5-6]. For the PMSGs, they are the most popular electrical machines for the direct drive wind turbines .they benefit with an excellent efficiency and energy yield [7]. In addition, the permanent magnets PM replace the excitation circuits in the rotor so it assures a permanent magnetic field. Therefore, the maintenance in the rotor are removed and the efficiency is improved.

In this paper, four models are treated. Several disciplines existing within the turbine are taken into account. Mechanical model processes the parameters of the dynamic behavior of the wind turbine to predict the torque generated at the turbine shaft from the kinetic torque of the wind. Geometric Model Allows to have a feasible structure for the design and analysis of the system. Magnetic model illustrates the influence of the permanent magnets by producing a permanent magnet flux within the machine. Electrical model determine the characteristics and the parameters of the generator. The relevance of the elaborated models is tested by the design in 2D of the PMSG with the MATLAB-FEMM software and the study of the system electromagnetic behavior by the finite element method FEM.

II. CURRENT STATUS OF WIND ENERGY IN THE WORLD ENERGY PLAN

In recent years the exploitation of wind energy power is increasing. It is exploited since antiquity and has underwent a boom in the latest thirteen years since the oil shocks. In fact, according to the statistics of the International Energy Agency IEA, the global energy consumption from wind power has increased from 3.4 TWh in 1990 to 790 TWh in 2016 [8]. In an other hand, the statistics given by the World Wind Energy Association WWEA, mentioned in "Figure 1", show that the global capacity of wind farms is changing annually from 435.284 GW in 2015 to reach 744 GW in 2020 [9]. This capacity has provided 7% of global demand for electricity in 2020 [9]. In fact, the wind Turbine Installations in 2020 have an energy capacity of 93 GW equivalent to 50% more than in 2019 and more than ever installed in one year [9].

IEECP'21, July 29-30, 2021, Silicon Valley, San Francisco, CA – USA

DII: https://sci-index.com/DAI/2021.99101/IEECP/16366077

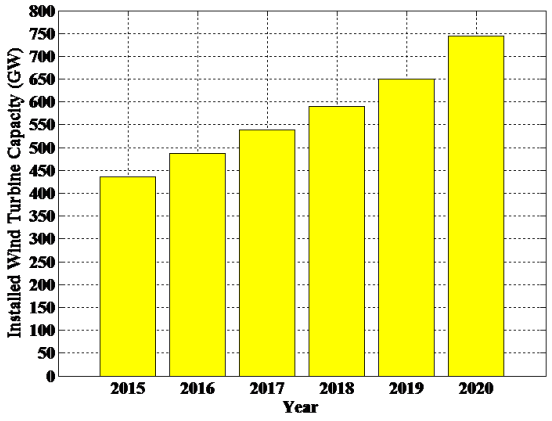

Figure 1. The Evolution of Installed Wind Turbines Capacity between years 2015 and 2020

Many regions from the advanced nations had the courage to invest in the installation of wind Turbines. The WWEA followed up the evolution of installed wind turbines in different zone between 2018 and 2020 as clarified "Figure 2" [9]. By the way, China and United-States have achieved new records in wind turbines installation. For European countries, they show slight growth due to the coronavirus crisis which has caused supply chain disruptions and luck of manpower.

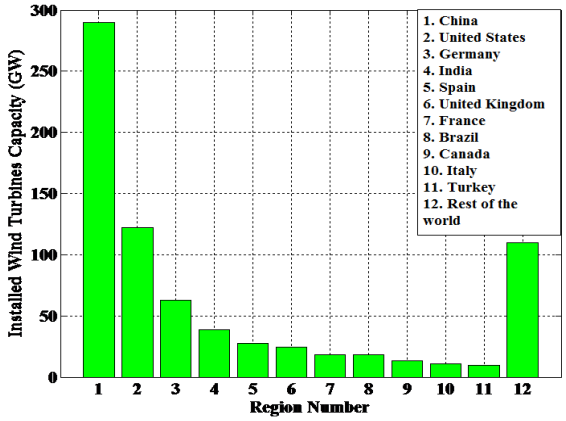

Figure 2. The Evolution of Installed Wind Turbines Capacity in different regions in 2020

A report of Global Wind Energy Council GWEC affirms that experts consider the year 2021 to be decisive year in confronting the barriers imposed by global climate change caused by the carbon emission and the harmful waste for the ecosystem [10]. They claim that wind power is the most favorable source that offers the greatest amount of de-carbonization per MW. They encourage the global wind industry to be united to highlight the major role that can play this energy in overcoming the barriers that threaten the world evolution in the future.

III. WIND TURBINE MODELLING

The modelling of a wind turbine is an important issue especially in the elaboration of optimal design [11]. Therefore, the structure of the wind conversion chain to be modeled in the study is a simplified chain dedicated to small scale wind production as clarified "Figure 3". It is a horizontal-axis turbine with three blades coupled directly to a permanent magnet synchronous generator. This generator presents surface permanent magnets with radial flux glued to an inner rotor. The electrical energy produced is stored to a battery through a diode bridge rectifier. The direct transmission of the turbine torque to the generator rotor encounters 2 types of losses which are friction torque and inertia torque.

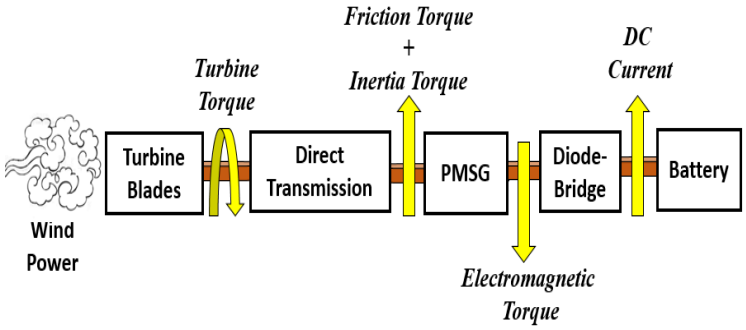

Figure 3. Simplified Wind Power Conversion Chain

A. Mechanical Model

Wind is the only variable that stimulate the mechanical movement of the turbine. It represents the only input variable of the turbine model. Its speed V_v in terms of time is described by a mathematical model. Referring to [12], an analytical wind model related to an urban site is given in "Equation 1" and represented in "Figure 4".

$$V\_v\,(t) = 10 + 0.2\sin(0.1047t) + 2\sin(0.2665t) + \sin(1.2930t) + 0.2\sin(3.6645t) \quad (1)$$

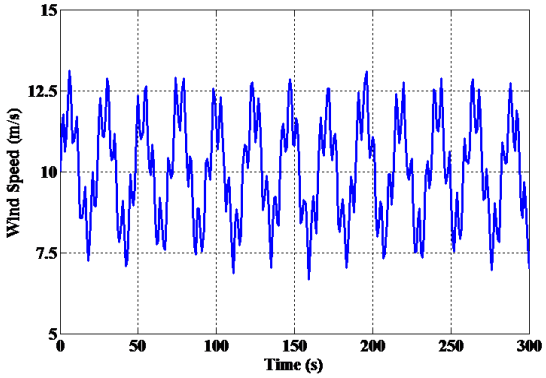

Figure 4. The Wind Profile as function of Time

The performance of the turbine in generating power is evaluated by the power coefficient C_p which represents the ratio of the power captured by the wind turbine and the kinetic power of the wind. For a setting fixed angle, the C_p analytical model of the commercialized BERGEY brand turbine is function of the reduced speed λ as expressed in "Equation 2".

$$C_p = -3{,}89.10^{-8}\lambda^7 - 4{,}21.10^{-6}\lambda^6 + 2{,}1.10^{-4}\lambda^5 - 3{,}1.10^{-3}\lambda^4 + 1{,}64.10^{-2}\lambda^3 - 1{,}76.10^{-2}\lambda^2 + 1{,}74.10^{-2}\lambda - 1{,}93.10^{-3} \quad (2)$$

The tip speed ratio λ, as defines "Equation 3", is the ratio of the tangential speed at the end of the blade $R_T\Omega$ to the instantaneous wind speed V_v. The blade radius of the chosen turbine R_T is equal to 1.25m [12-13].

$$\lambda = \frac{R_T \Omega}{V_v} \quad (3)$$

According to C_p curve mentioned in "Figure 5", the power Turbine reaches its maximum for the optimal values of $C_{p.opt}$ equal to 0.442 and $\lambda_{p.opt}$ equal to 6.9.

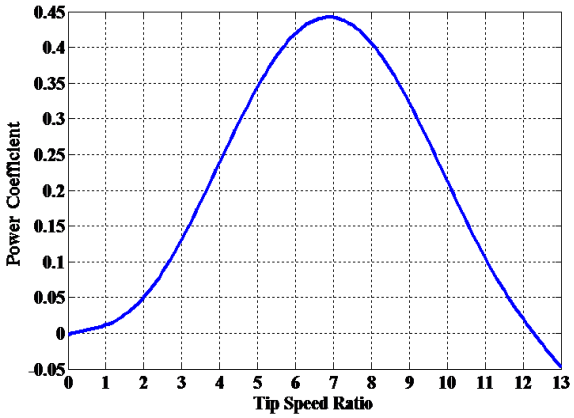

Figure 5. Aerodynamic Power Coefficient with respect to the Tip Speed Ratio

The associated wind turbine power P_T is defined as [14-15]:

$$P_T = \frac{1}{2}\rho S_T C_p(\lambda) V_v^{\,3} \quad (4)$$

With ρ the air density (Kg.m-3) and S_T represents the surface swept by the turbine blades (m^2).

The surface of the turbine S_T differs depending on its type. For horizontal axis wind turbines, the area swept by the blades is given as follows.

$$S_T = \pi R_T^{\,2} \quad (5)$$

The intervention of the angular rotation speed Ω of the rotor shaft product a turbine torque T_T illustrated in "Equation 6" [14-15].

$$T_T = \frac{P_T}{\Omega} = \frac{\frac{1}{2}\rho R S_T C_p(\lambda) V_v^{\,2}}{\lambda} \quad (6)$$

The characteristics of the turbine through the power extraction curves are shown in "Figure 6" as a function of the rotation speed Ω for different wind values included in the wind interval admissible for the turbine blades drive.

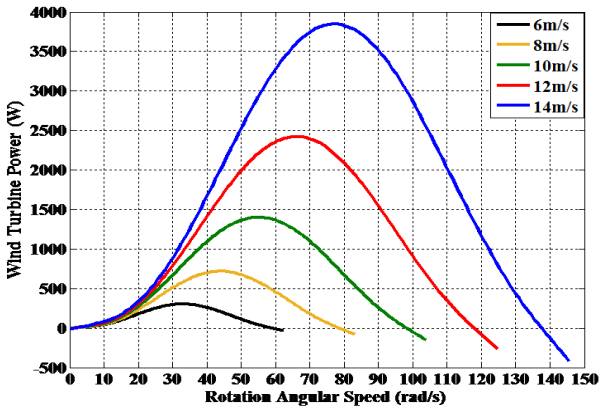

Figure 6. Wind Turbine Power vs. Rotation Angular Speed

The dynamic coupling characterizing the turbine-Generator mechanical behavior is given by the empirical "Equation 7" relating the turbine torque T_T and the electromagnetic torque T_{em} with the rotation angular speed Ω, the turbine inertia J_T and the generator friction coefficient f_m.

$$T_T - T_{em} = J_T \frac{d\Omega}{dt} + f_m \Omega \quad (7)$$

B. Geometric Model

The geometric part of the turbine is summed up in the design of the blades and the generator.

1)Blades Geometric Model

The studied turbine consists of 3 blades located on a horizontal axis sweeping a circular surface shown in "Figure 7" and equal to:

$$S_T = \pi R_T^{\,2} \quad (8)$$

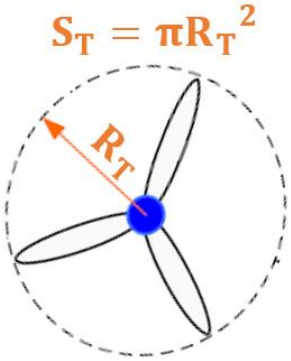

Figure 7. Geometric Model of the turbine Blades

2)PMSG Geometric Model

The principle of this methodology is based on fixing the electromagnetic torque of the generator imposed by the rotor turbine on the nominal value. According to the relation given in "Equation 9", the bore radius r_s will be calculated and geometric parameters are deduced [12]. This equation connect the fixed electromagnetic torque T_{em} of the generator with its bore radius r_s, its active length l_r, the magnet fundamental induction peak value B_{1a} and the linear current effective value K_{1s} [12-14]

$$T_{em} = 2\pi r_s l_r B_{1a} K_{1s} \quad (9)$$

The machine length l_r is given as follow [12-15]

$$l_r = \frac{r_s}{R_{rl}} \quad (10)$$

With R_{rl} is a virtual parameter chosen according to the designer expertise.

The generator air gap g is deduced from the empirical relation under below [12-15].

$$g = 0.001 + 0.003\sqrt{r_s l_r} \quad (11)$$

The angular width of the magnet per pole w_m is calculated as mentioned in "Equation 12". For the magnet thickness l_m, it is deduced as shown in "Equation 13" [12-15].

$$w_m = \frac{2\ \alpha_{magnet}}{p}\ r_s \quad (12)$$

With p is the number of the generator pole pairs and α_{magnet} is the magnet angle.

$$l_m = K_c g\ \frac{\mu_r}{B_r/B_a - 1} \quad (13)$$

With K_c is the crankcase coefficient, μ_r is the magnet's relative permeability, B_a is the induction magnet peak value in the air-gap and B_r is the magnet's remanent induction.

To simplify the design process, the stator and rotor depth, d_y and d_r, have equal values which is the same case for the slot and tooth width, w_s and w_T. [12-15]. The expressions of these graders are given in "Equation 14" to "Equation 15".

$$d_y = d_r = \frac{r_s\ B_a}{p\ B_y}\ \alpha_{magnet} \quad (14)$$

Where B_y represents the induction in the stator yoke.

$$w_s = w_T = \frac{4\pi r_s}{3N_{slots}} \quad (15)$$

With N_{slots} is the slots number.

The slot trapezoidal shape is presented in "Figure 8" having a depth d_s given in "Equation 16" [15]

$$d_s = R_{dr} r_s \quad (16)$$

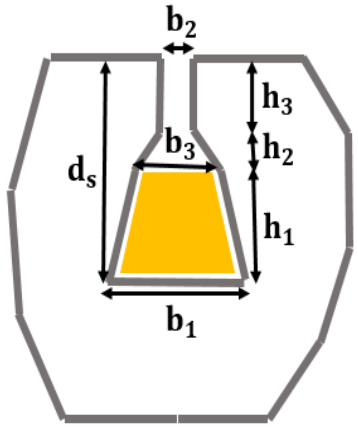

Figure 8. Characteristics of the trapezoidal slot

With:

$$\begin{cases} h_3 = 0.02 r_s & b_1 = w_s \\ h_2 = \frac{w_s}{8} & b_2 = \frac{w_s}{2} \\ h_1 = d_s - h_2 - h_3 & b_3 = \frac{3w_s}{4} \end{cases}$$

C. Magnetic Model

Permanent magnets cause the presence of a permanent magnet field in the air gap of the PMSG. In fact, the magnet fundamental induction peak value B_{1a} is expressed in "Equation 17" as function of the magnet angle α_{magnet} and the induction magnet peak value in the air gap B_a [12].

$$B_{1a} = \frac{4}{\pi} B_a \sin(\alpha_{magnet}) \quad (17)$$

The magnet angle α_{magnet} is a function of the filling factor of the pole K_p as mentioned bellow [12].

$$\alpha_{magnet} = \frac{4}{\pi} K_p \quad (18)$$

The induction magnet peak value in the air gap B_a is given as follows [12].

$$B_a = B_r \frac{l_{m/\mu r}}{K_c\, g + l_{m/\mu r}} \quad (19)$$

The vacuum magnetic flux received by a stator phase for a single conductor per slot Φ_{s1} is expressed as mentioned in "Equation 20" [12-14].

$$\Phi_{s1} = 2K_b N_{spp} B_{1a} r_s l_r \quad (20)$$

The total vacuum magnetic flux generated in a stator phase, expressed in "Equation 21", is function of the conductor number per slot N_{cs} [12-14].

$$\Phi_s = N_{cs} \Phi_{s1} \quad (21)$$

D. Electrical Model

The electrical part of the wind turbine lies in the electromagnetic behavior of the generator. The calculation of the electrical graders is based on the geometric model of the considered machine.

The linear current effective value K_{1s} characterizes the current distributed along the air gap per unit of length. It depends, as cited in "Equation 22" on the surface density of the current J_s, the tooth width w_T, the slot width w_s, the slot depth d_s, the winding factor K_{B1} and the slot filling coefficient K_r [12].

$$K_{1s} = \frac{J_s w_s d_s}{w_s + w_T} K_{B1} K_r \quad (22)$$

The winding factor K_{B1} is limited to the fundamental term of the distribution factor K_{z1}. It is deduced from the number of slots per pole and per phase N_{spp} as clarified in "Equation 23" [12].

$$K_{z1} = K_{B1} = \left| \frac{\sin\left(\frac{\pi}{6}\right)}{N_{spp} \sin\left(\frac{\pi}{6N_{spp}}\right)} \right| \quad (23)$$

The slot filling factor K_r is characterized by the ratio between the slot surface actually filled with copper S_{copper} and the total slot surface S_{slot} as given in "Equation 24" [12].

$$K_r = \frac{S_{copper}}{S_{slot}} \quad (24)$$

Therefore, the magnetizing inductance L_{m1} , the leakage inductance L_{f1}, the mutual inductance between stator phases M_{s1}, the generator phase inductance L_{s1}, and the electrical resistance for a phase R_{s1} are explained for a single conductor per slot as follow in equations below [12-14].

$$L_{m1} = \frac{4\mu_0 l_r r_s}{\pi(K_c g + l_m)} {N_{spp}}^2 {K_{B1}}^2 \quad (25)$$

$$L_{f1} = 2\mu_0 l_r p N_{spp} \lambda_{slot} \quad (26)$$

$$M_{s1} = \frac{-L_{m1}}{2} \quad (27)$$

$$L_{s1} = L_{m1} - M_{s1} + L_{f1} \quad (28)$$

$$R_{s1} = 2\rho_{copper}\left[l_r + \frac{\pi^2(r_s + 0.5d_s)}{2p}\right]\frac{pN_{slots}}{\pi r_s d_s K_r} \quad (29)$$

The current in stator windings for a single conductor per slot I_{s1} is function of the current density J_s as shows "Equation 30" [15].

$$I_{s1} = \frac{J_s d_s K_r \pi r_s}{6pN_{spp}} \quad (30)$$

The vacuum electromotive force E generated in the stator windings is given by "Equation 31" [12].

$$E = p\Omega\Phi_s \quad (31)$$

With Ω is the rotational angular speed of the generator rotor.

The study is devoted to three-phase generator delivering on an alternating voltage source of maximum amplitude V_{dim}. For the case referred to in this paper, the voltage source delivers to a battery of accumulators with voltages V_{bat} through a diode bridge. Consequently, V_{dim} is related with V_{bat} as expressed in "Equation 32" [12].

$$V_{dim} = \frac{2}{\pi} V_{bat} \quad (32)$$

The generative operation of the machine is described by the fundamental "Equation 33". Therefore, the Fresnel Diagram is obtained at the base dimensioning point as illustrated in "Figure 9". In fact, the base dimensioning point is characterized by the sizing voltage V_{dim}, electrical angular speed ω_{dim}, and electromagnetic design torque T_{em_dim} [12-14].

$$\underline{E} = \underline{V_{dim}} + R_s\underline{I_s} + j\,L_s\omega_{dim}\underline{I_s} \quad (33)$$

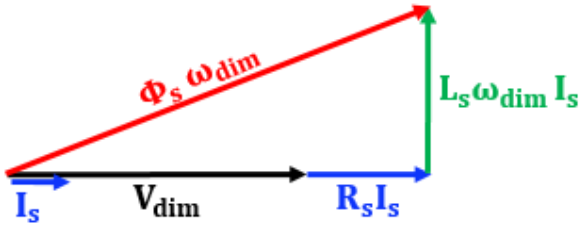

Figure 9. Generator Fresnel Diagram at Base Point

The purpose of this diagram is to calculate the number of conductors per slot N_{cs}. Indeed, the generator electrical parameters are a function of the number of conductors per slot and the calculated graders for a single conductor per slot as mentioned in equations bellow [12-14].

$$L_f = {N_{cs}}^2 L_{f1} \quad (34)$$

$$L_m = {N_{cs}}^2 L_{m1} \quad (35)$$

$$L_s = {N_{cs}}^2 L_{s1} \quad (36)$$

$$R_s = {N_{cs}}^2 \quad (37)$$

$$I_s = \frac{I_{s1}}{N_{cs}} \quad (38)$$

As a conclusion, the number of conductors in a single slot is obtained by solving the quadratic "Equation 39" obtained by replacing the electrical quantities expressions developed above in the formula spelled out from generator electrical diagram of "Figure 8".

$$ {N_{cs}}^2 - \frac{2V_{dim}R_{s1}I_{s1}}{(\Phi_{s1}\omega_{dim})^2 - [{R_{s1}}^2 + (L_{s1}\omega_{dim})^2]{I_{s1}}^2} N_{cs} - \frac{{V_{dim}}^2}{(\Phi_{s1}\omega_{dim})^2 - [{R_{s1}}^2 + (L_{s1}\omega_{dim})^2]{I_{s1}}^2} = 0 \quad (39)$$

IV. FINITE ELEMENT ANALYSIS OF THE PMSG

In order to design the generator in 2D, a MATLAB-FEMM code is elaborated. This code has as input parameters geometric graders resulting from structural model of the machine. The main target of this part is to evaluate the performance of the interconnected models. For a reference machine with electromagnetic torque of 27.5 N.m, the bore radius is equal to 83.2 mm. The obtaining of the bore radius value is due to expertise of the designer in design of electrical machines and basing on several hypothesis. In fact, simplifying hypotheses are cited. At first, the filling factor K_p is chosen equal to 0.833. Thus, the angular width of the magnet α_{magnet} is equal to 75°. Such a value minimize the harmonics of the electromotive force EMF and ensure a good ratio between the volume of the magnet and the effective value of the induction in the air gap [12, 15]. The slot fill factor K_r is fixed to 0.35. The permanent magnets used are Neodymium Iron Boron Magnets NdFe30 having residual magnetization B_r equal to 1.1 T and relative permeability μ_r equal to 1.05. Subsequently, generator characteristics coming from analytical models are calculated.

As a result, the 2D geometric model of the reference machine is obtained by finite element software FEMM. It is represented in "Figure 10" having 36 trapezoidal slots with 47 conductors per slot and 12 magnets. All parameters of the reference machine are given in the table in the appendix.

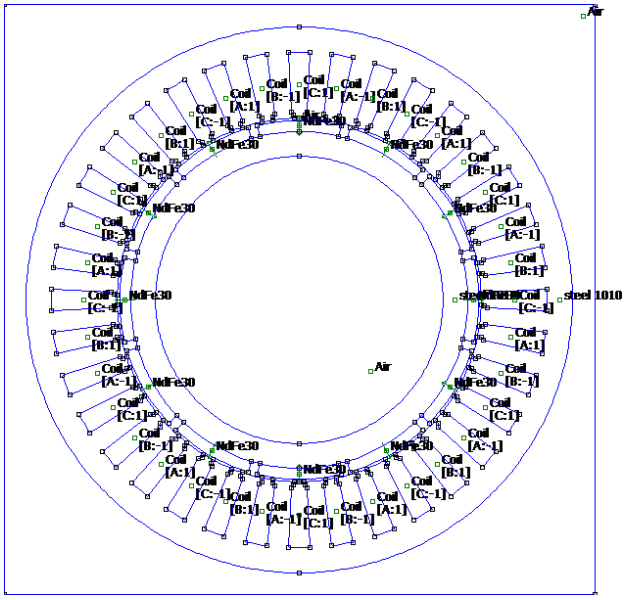

Figure 10. 2D Geometric Model of the PMSG with FEMM.

The induction variation B_a in the air-gap is shown in "Figure 11". Its peak value is 0.9 T. It is close to the analytical value 0.846 T.

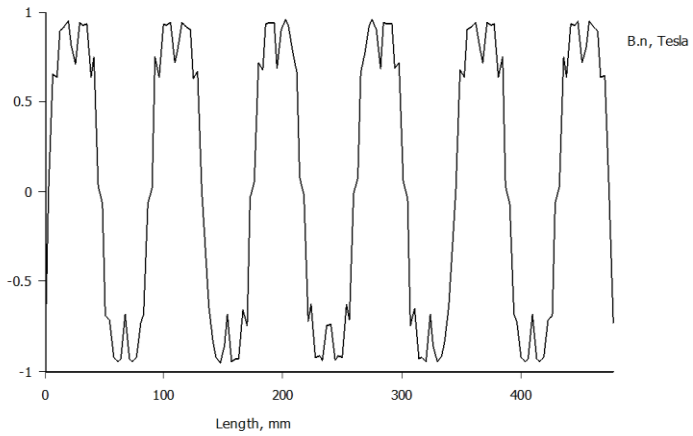

Figure 11. Induction as function of the air-gap perimeter length.

The magnetic field lines generated by the rotation of the permanent magnets glued to the rotor are represented in the stator and rotor yoke as mentioned in "Figure 12".

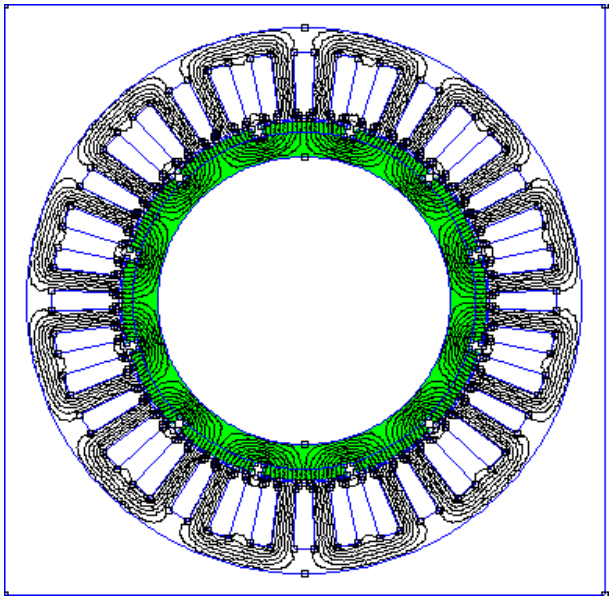

Figure 12. Field Lines Distribution in the PMSG.

The rotational movement of the magnets-rotor assembly highlighted in green in "Figure 12" is generated by the rotational movement of the turbine. According to the induction phenomena, an induced electromotive force EMF and an induced current in the three phase's stator windings. There will be a generation of an electromagnetic torque. For the studied case, the electromagnetic torque curve obtained by the finite element method with MATLAB-FEMM software is represented in "Figure13". Its average value is equal to 23.5 N.m. Comparing to 27.5 N.m, a tolerable error of 17% is introduced between analytical and numerical results given the smoothness of the finite element analysis approach and considering the effect of the winding type.

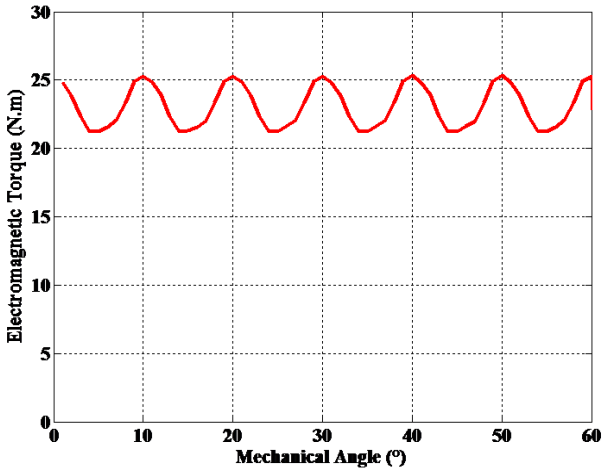

Figure 13. Electromagnetic Torque Curve Obtained by the Finite Element Method

The simulation results curves allow the validation of the PMSG analytical models. The feasible structure of the machine proved the reliability of the geometric model. The induction curve and the safe distribution of the field lines in the machine confirmed the magnetic model. Indeed, the average value of the electromagnetic torque is at the base of the determination of the parametric modelling of the whole chain. Such curve look and value support the analytical approach for the modeling of the wind turbine chain. Therefore, the analytical models are validated.

V. CONCLUSION

In this paper, a modelling method of a wind chain is described. The analytical resolution of the mechanical-geometric parameters of the airfoils, the geometric sizes of the PMSG and the calculation of the electrical and magnetic graders allows the parameterized evaluation of the wind power conversion chain. The performance of the generator are tested with the finite element analysis using MATLAB-FEMM software. A 17% error between analytical and numerical value of the electromagnetic torque of the PMSG is tolerable given the reliability of the considered method. As a perspective, models are suitable for the elaboration of an optimization model of the wind turbine to product optimal design to the wind market.

VI. Appendix

The attached table summarizes the Characteristics of the reference machine used in the case studied.

Machine Parameter	Unit	Value
r_{dr}	--	0.366
r_{rl}	--	2.025
J_s	A/mm^2	2.7
p	--	6
B_y	T	1.4
N_{spp}	--	1
Ω_{dim}	rad/s	40
r_s	mm	83.16
l_r	mm	41.06
w_m	mm	36.28
g	mm	1.17
l_m	mm	4.94
w_s	mm	9.68
d_y	mm	11.3
d_s	mm	30.44

VII. REFERENCES

[1] M. Santosh, C. Venkaiah and D. M. V. Kumar, "*Current Advances and Aproaches in Wind Speed and Wind Power Forecasting for Improved Renewable Energy Integration: A Review",* Engineering Reports, 2(6), April 2020.

[2] A F Reines and B Svingen, *"Analysis and Improvement of a Mathematical Turbine Model",* Journal of Physics: Conference Series, Vol. 1608, March 2020.

[3] C H Chong, A R Rigit and I Ali, *"Wind Turbine Modelling and Simulation Using MATLAB-SIMULINK",* IOP Conference Series: Materials Science and Engineering, October 2020.

[4] L Golebiowski, M Golebiowski, D Mazur and A Smolen, *"Analysis of Axial Flux Permanent Magnet Generator"*, The International Journal for Computaion and Mathematics in Electrical and Electronic Engineering, January 2020.

[5] A. Hemeida, P. Sergeant, A. Rasekh and J. Vierendeels, *"An Optimal Design of a 5MW AFPMSM for Wind Turbine Applications Using Analytical Model",* 2016 XXII International Conference on Electrical Machines, DOI: 10.1109/ICELMACH.20167732691.

[6] K. Latoufis, A. Rontogiannis, V. Karatasos, P. Markopoulos and N. Hatziargyriou, *"Thermal and Structural Design of Axial Flux Permanent Magnet Generators for Locally Manufactured Small Wind Turbines",* 2018XIII International Conference on Electrical Machines, pp. 2381-4802, September 2018.

[7] K.Sindhya, A. Mannien, K. Miettinen and J. Pippuri, *"Design of permanent magnet synchronous generator using interactive Mulitiobjective optimization"*, IEEE Transactions on Industrial Electronics, vol. 64, pp. 9776-9783, December 2017.

[8] World Energy Outlook, iea.org.

[9] World Wind Energy Asociation, wwindea.org.

[10] Global Wind Energy Council, gwec.net.

[11] L. Gang, Z. Hanguo, G. Youguang, L. Chengcheng and M. Bo, *"A Review of Design Optimization Methods for Electrical Machines"* , Energies, November 2017.

[12] D. Tran, "*Conception Optimale Intégrée d'une chaine éolienne « passive » : Analyse de robustesse et validation expérimentale", National Institute o Polytechnic of Toulouse*, 2010.

[13] N. Ben Halima, S. Ammous and A. Walha, *" Constant-Power Management algorithms of a hybrid wind energy system"*, Journal of Renewable and Sustainable Energy, October 2018.

[14] A. Abdelli, *"Optimisation Multicritère d'une chaine éolienne passive"*, National Institute o Polytechnic of Toulouse, 2007.

[15] B. Sareni, A. Abdelli, X. Roboam and D.H. Tran, *"Model simplification and optimization of a passive wind turbine generator",* Renewable Energy, vol. 34, p. 2640-2650, April 2009.